Study of the 6.05 MeV cascade transition in C 12 (α , γ) O 16

ARTICLE *in* FUEL AND ENERGY ABSTRACTS · SEPTEMBER 2011

DOI: 10.1016/j.physletb.2011.08.061

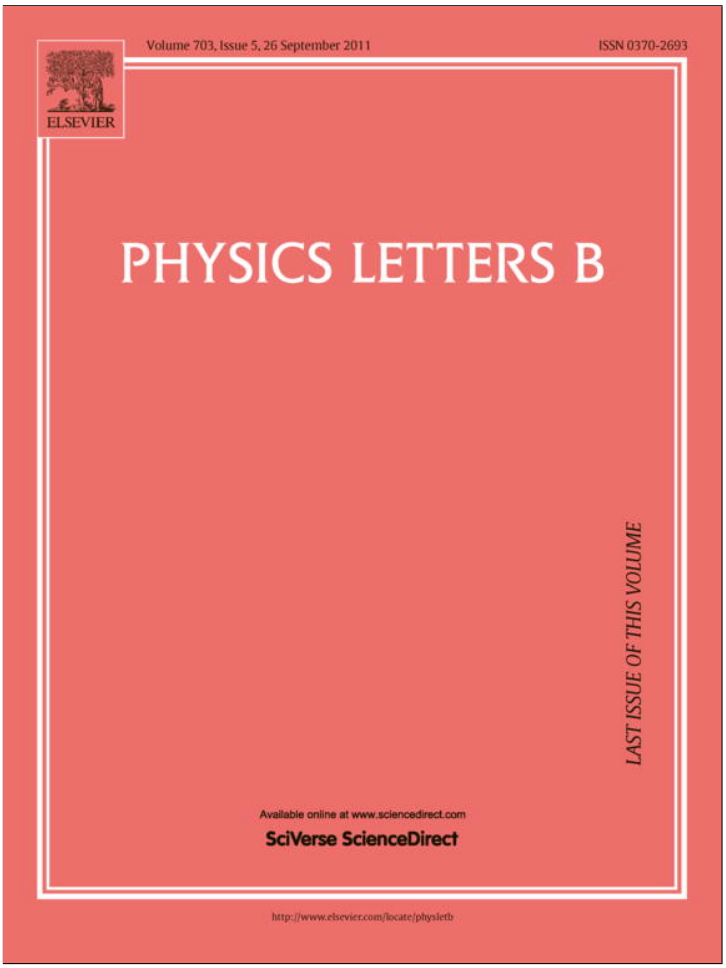

Physics Letters B 703 (2011) 557–561

Contents lists available at SciVerse ScienceDirect

Physics Letters B

www.elsevier.com/locate/physletb

Study of the 6.05 MeV cascade transition in $^{12}C(\alpha,\gamma)^{16}O$

D. Schürmann [a,b], A. Di Leva [b,c], L. Gialanella [b,d], R. Kunz [a,1], F. Strieder [a,*], N. De Cesare [b,d], M. De Cesare [b,d], A. D'Onofrio [b,d], K. Fortak [a,1], G. Imbriani [b,c], D. Rogalla [a,1], M. Romano [b,c], F. Terrasi [b,d]

[a] Institut für Experimentalphysik, Ruhr-Universität Bochum, D-44780 Bochum, Germany
[b] Istituto Nazionale di Fisica Nucleare (INFN), Sezione di Napoli, I-80126 Napoli, Italy
[c] Dipartimento di Scienze Fisiche, Università Federico II, I-80126 Napoli, Italy
[d] Dipartimento di Scienze Ambientali, Seconda Università di Napoli, I-81100 Caserta, Italy

ARTICLE INFO

Article history:
Received 26 July 2011
Received in revised form 21 August 2011
Accepted 21 August 2011
Available online 25 August 2011
Editor: V. Metag

Keywords:
Nuclear astrophysics
Helium burning
α-Capture reaction
Cascade transition

ABSTRACT

The radiative capture reaction $^{12}C(\alpha,\gamma)^{16}O$ has been investigated in the energy range $E = 3.3$ to 4.5 MeV. This experiment focused in particular on the cascade transition to the 0^+ state at $E_x = 6.05$ MeV in ^{16}O and was performed by detecting the capture γ-rays with a NaI detector array at the windowless ^4He gas target of the recoil mass separator ERNA in coincidence with the ^{16}O ejectiles. The 6.05 MeV transition has been considered recently as a component accounting for up to 15% of the $^{12}C(\alpha,\gamma)^{16}O$ total cross section at astrophysical energies. The arrangement of the detector array yielded additional information on the γ-ray multipolarity, i.e. the ratio σ_{E2}/σ_{E1}, and it was found that the 6.05 MeV transition is entirely E2 in the studied energy range. The results for this transition are analyzed in an R-matrix formalism and extrapolated to the relevant Gamow energy of stellar helium burning, $E_0 \simeq 300$ keV. In contrast to a previous analysis, the present extrapolation suggests a negligible contribution from this amplitude, $S_{6.05}(300) < 1$ keV b. Additional data for cascade transitions to excited states at $E_x = 6.13$, 6.92, and 7.12 MeV, respectively, as well as to the ground state were obtained and the corresponding S factors in the studied energy range are given.

1. Introduction

After stellar hydrogen burning, the core of a star is transformed mainly to ^4He. Without the core energy production, the center contracts, and the core temperature, T_C, rises. Meanwhile the outer layers of the star expand and the star develops into the Red Giant phase. At $T_C > 10^8$ K the nuclear energy production, due to the synthesis of three α particles to carbon (triple-α process), becomes large enough to sustain the temperature of the core. As a consequence, the contraction stops and the helium burning phase is started. In the first stage of stellar helium burning – since the ^{12}C abundance is very low – the only active process is the triple-α reaction, while later after build up of a significant abundance of carbon the $^{12}C(\alpha,\gamma)^{16}O$ reaction is the dominating process. The cross section of the $^{12}C(\alpha,\gamma)^{16}O$ reaction at the relevant Gamow energy – $E_0 \simeq 300$ keV – determines the helium burning time scale and, together with the convection mechanism, the abundances of carbon and oxygen at the end of helium burning. The carbon abundance at that stage has important consequences for the subsequent evolution of various astrophysical scenarios, e.g. a direct influence on type II Supernova (SN) nucleosynthesis [1–5], the maximum luminosity and kinetic energy of type I SN [6], and the cooling sequence of CO white dwarfs [7–9]. Thus, an experimental determination of the $^{12}C(\alpha,\gamma)^{16}O$ cross section in the relevant energy region in the order of 10% or better will improve our understanding of the convection processes and remains an important ingredient for the understanding of stellar evolution.

The cross section of the reaction $^{12}C(\alpha,\gamma)^{16}O$ ($Q = 7.162$ MeV) is dominated by E1 and E2 capture processes into the ^{16}O ground state, where the two multipoles appear to be of similar importance at stellar energies. This energy region is not accessible with present experimental techniques and an extrapolation to E_0 is necessary. The cross section $\sigma(E)$ at low energies is typically expressed in terms of the astrophysical S factor [10] defined for this reaction as:

$$S(E) = \sigma(E) E e^{650.35/\sqrt{E}} \tag{1}$$

where E is in keV. Since the capture cross sections of the E1 and E2 multipoles have different energy dependencies, one must have an independent and precise information on the energy dependence of each multipole cross section.

* Corresponding author.
E-mail address: strieder@ep3.rub.de (F. Strieder).
[1] Present address: RUBION, Ruhr-Universität Bochum, D-44780 Bochum, Germany.

0370-2693/$ – see front matter
doi:10.1016/j.physletb.2011.08.061

A series of direct experiments with γ-ray detector arrays (e.g. [11–15]) were carried out in the past years to constrain the ground state transitions. Additional information can be derived from measurements of the (α,α)-elastic scattering [16], the β-delayed α-decay of ^{16}N [17–19], and the total cross section with a recoil separator [20].

In addition to the ground state contributions, cascade transitions have to be considered whereas much less data are available. The cascade transitions can proceed through a number of ^{16}O excited states and in particular transitions to the $E_x = 6.92$ MeV ($J^\pi = 2^+$) and 7.12 MeV ($J^\pi = 1^-$) have been observed in the past [21,22].

A more detailed discussion of the various contributions is given for example in the review of Buchmann and Barnes [23] where a total S factor of $S(300) = 145$ keV b is recommended with an uncertainty range of 25 to 35%.

Recently, the importance of the $J^\pi = 0^+$ state at $E_x = 6.05$ MeV in ^{16}O was emphasized [24]. This excited 0^+ state decays exclusively by e^+e^- transition (E0) to the 0^+ ground state and only the primary γ-ray line can be observed. This component was measured with the DRAGON recoil separator at TRIUMF, Canada, in the energy[2] region $E = 2.22$ to 5.42 MeV with a high efficiency BGO γ-ray array in coincidence with the observed recoils. The data have been analyzed with an R-matrix calculation and extrapolated to the astrophysical energy region, $S_{6.05}(300) = 25^{+16}_{-15}$ keV b. This value is an additional contribution to the $S(300)$ given in [23] and, thus, a non-negligible part of the total S factor at helium burning temperatures. Therefore, this cascade transition deserves a further investigation in order to prove its importance for stellar evolution.

The DRAGON experiment [24] spanned a rather large energy interval and is, due to the coincidence condition, one of the first reliable γ-ray measurements above $E > 3$ MeV in ^{12}C$(\alpha,\gamma)^{16}$O. In general data at high energies are important for reliable R-matrix extrapolations to astrophysical energies, but the only existing direct γ-ray measurement at such energies so far was published in 1964 [25] where a quoted absolute uncertainty of a factor 2 prevents any definite conclusion. However, the DRAGON measurement [24] suffered from low ^{12}C beam intensities, the moderate energy resolution of the BGO crystals, and the limited acceptance of the separator preventing an independent normalization to the ^{12}C$(\alpha,\gamma)^{16}$O ground state transition. Some of these issues could be overcome in the measurement reported here.

2. Experimental setup

The experiment was carried out at the ERNA (European Recoil Separator for Nuclear Astrophysics) recoil separator at the Dynamitron – Tandem Laboratory of the Ruhr-Universität Bochum, Germany. A ^{12}C beam intensity of typically 5 pμA in the 3^+ or 4^+ charge state was used in the energy range $E = 3.3$ to 4.5 MeV. Details of the experimental setup are as reported previously [26–28]. Briefly, a ^{12}C ion beam emerging from the tandem accelerator was focused by a quadrupole doublet, filtered by a 52° analyzing magnet, and guided into the 75° beam line of ERNA by a switching magnet. A quadrupole doublet after the switching magnet was used to focus the beam onto a ^{4}He windowless gas target. The inner gas cell had a length of 40 mm and an areal density of 4×10^{17} atoms/cm^2. A Wien filter before the analyzing magnet and another before the gas target provided the necessary ion beam purification from recoil-like contaminants [29]. The number of projectiles impinging on the target was determined through the elastic scattering yield observed in two collimated silicon detectors located in the target chamber at 75° with respect to the beam axis. After the gas target, the separator consisted sequentially of the following elements: a quadrupole triplet, a Wien filter, a quadrupole singlet, a 60° dipole magnet, a quadrupole doublet, a Wien filter, and the ΔE–E recoil detector. Finally, several steerers, Faraday cups, and slit systems were installed along the beam line for diagnostic purposes.

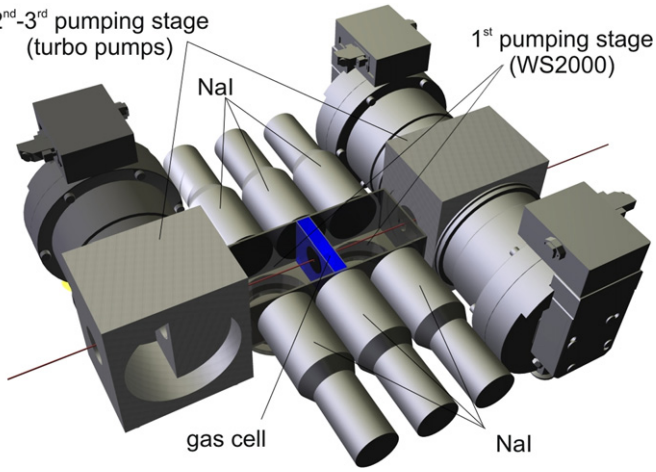

Fig. 1. Gamma-ray detection array at the ERNA windowless gas target. In the sketch the inner chamber is opened and the gas cell is visible. The two WS2000 roots blowers below the gas target pumping the inner cell are not shown, while for the next stages the TMH521 turbo pumps are depicted. For clarity, one TMH 521 has been removed.

The experimental procedures were basically identical to the measurement of the total cross section of ^{12}C$(\alpha,\gamma)^{16}$O with this setup reported in [20]. The ERNA separator had full angle and energy acceptance along the length of the gas target for the ^{16}O recoils, i.e. emitted from ground state and cascade transitions of ^{12}C$(\alpha,\gamma)^{16}$O, over the entire energy range of the present experiment [28]. The γ-ray detection system was similar to the configuration used for the ^{3}He$(\alpha,\gamma)^7$Be measurement [30] described in [31]: 6 identical $3'' \times 3''$ NaI detectors. The NaI detectors were oriented perpendicular to the beam axis with a front face distance of 60 mm and 3 detectors on each side of the windowless gas target, as shown in Fig. 1.

The data acquisition was based on a mixed FAIRVME bus [32]. The spectra of the NaI detectors and the ΔE–E telescope were controlled on-line, while the raw data were saved event-by-event on hard disk for an off-line data analysis.

3. Data analysis

The trigger of the acquisition system was based on the signal from the end-detector. Therefore, only γ-ray events in coincidence with recoil-like signals have been acquired. The selection of the appropriate ΔE–E region for the ^{16}O recoils set further strong constraints on the identification of γ-ray events from the ^{12}C$(\alpha,\gamma)^{16}$O reaction. The background from accidental coincidences between γ-rays and recoil events in this ΔE–E region was estimated from γ-ray-recoil coincidences of the ^{12}C contaminants in the ΔE–E matrix. This background was found to be negligible at $E_\gamma > 3$ MeV, i.e. the spectra were basically background free.

The γ-ray spectra were energy calibrated separately for each detector. For this purpose radioactive γ-ray sources, ^{137}Cs and ^{60}Co, and the ^{12}C$(\alpha,\gamma)^{16}$O ground state transition were used. During the course of the experiment the energy calibration was also checked with the γ-ray lines from the ^{27}Al$(p,\gamma)^{28}$Si reaction. Both

[2] All energies are given in the center-of-mass frame except where quoted differently.

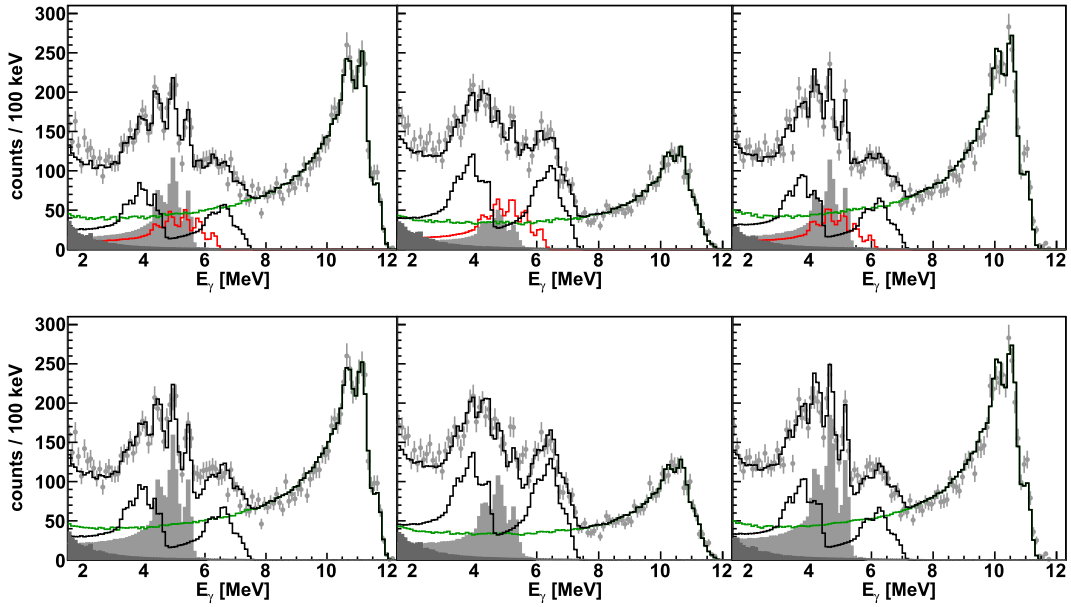

Fig. 2. Comparison of the γ-ray spectra at $E = 4.2$ MeV (filled circles) with the results of the fit for the different contributions: total = black line, 6.05 MeV transition = light gray shaded area, 6.13 MeV = red line, 6.92 + 7.13 MeV = lower black line, ground state = dark green line, background = dark shaded area. The lower panels show the analysis with the 6.13 MeV cascade amplitude fixed to zero ($\chi^2_{\rm red} = 2.33$), while in the upper panels this amplitude is a free fit parameter ($\chi^2_{\rm red} = 1.06$). In each row the upstream (left), central (middle), and downstream (right) detector pairs are shown. For clarity, the transitions to 6.92 and 7.12 MeV are displayed together, although they have been fitted separately. (For interpretation of the references to color in this figure legend, the reader is referred to the web version of this Letter.)

calibrations were found to be in good agreement. Different energy binnings of the raw spectra were tested and a final bin size of 100 keV was selected as a good compromise between energy resolution and statistics per bin. No systematic effect on the analysis was observed. After calibration the spectra of the detector pairs facing each other on both sides of the beam line were summed and three spectra could be analyzed per energy data point, called in the following downstream, central, and upstream spectrum, respectively.

The analysis of the γ-ray spectra was based on a GEANT4 [33] simulation. The GEANT4 simulation included the experimental setup with the NaI detectors and the target chamber. The origin of the simulated γ-ray events was distributed along the beam axis according to the measured gas pressure profile [34]. The simulated γ-ray energies were calculated from reaction energy, recoil energy loss, and Doppler shift effects. The experimental detector energy resolution (8% at $E_\gamma = 1$ MeV) was used to extract a realistic spectrum. However, the total energy resolution was mainly determined by Doppler shift. A set of simulated spectra was created for each energy and included primary and secondary transition through the 6.13, 6.92, and 7.12 MeV states in ^{16}O. In order to take into account the angular distribution of each transition all simulated spectra were calculated independently for the three detector pairs. Since a constant primary to secondary ratio of 1 was maintained in the analysis 5 scaling parameters had to be fitted for each transition. This analysis procedure is based on the fact that the present setup is suitable for an angle integrated measurement of the cross section as has been shown previously [31]. The ground state transition and the transition to the 6.05 MeV 0^+ state – primary only – were treated differently since a strong angular distribution is expected. E1 and E2 angular distributions have been simulated separately allowing for an adjustment of the E2/E1 ratio through the scaling parameters. At energies above $E = 4$ MeV interference effects in the angular distribution were included and calculated according to Barker and Kajino [35] using phase shifts from [16]: again the E2/E1 ratio and the absolute strength were determined experimentally. The effects of γ–γ angular correlations are expected to be small and, therefore, have been neglected in the simulation. The uncertainty of the simulation for the present setup was estimated to 5% from comparison of source measurements and GEANT4 simulation [31].

Finally, the simulated spectra of all transitions were combined in a simultaneous fit to the 3 experimental spectra at each beam energy. The data were fitted in the region $E_\gamma = 3.0$ to 7.6 MeV while at higher γ-ray energies only the integral of the ground state transition was considered. The Maximum Likelihood method for binned histograms was used in order to avoid biased results due to the low statistics of the measurement. Altogether 19 parameters were fitted in this procedure leading to 125 degrees of freedom (ndf) in the fit for the bin size used here. The equivalent χ^2 value was calculated for the best fit to allow a comparison of the results.

The best fit to the experimental spectra was obtained including contributions from all cascade transitions, i.e. through 6.05, 6.13, 6.92, and 7.12 MeV states as well as the ground state. A series of sample spectra at $E = 4.2$ MeV with the corresponding best fits is shown in Fig. 2. The sizable contribution of the 6.13 MeV transition (Fig. 2 upper panels) is in contrast to the results of the DRAGON analysis [24] where only a sporadic appearance of this transition with no significant influence was observed.[3] We repeated the analysis setting the 6.13 MeV amplitude to zero in order to compare the present results to the findings of [24]. The difference between the two approaches, i.e. analysis with and without a 6.13 MeV amplitude, turned out to be always more than 5 standard deviations of the corresponding χ^2 distribution (ndf = 125). The effect of the different analysis is demonstrated in Fig. 2, where the lower panels show the best fit without 6.13 MeV amplitude ($\chi^2_{\rm red} = 2.33$) while the upper panels include the fit of this contribution ($\chi^2_{\rm red} = 1.06$). From these results we conclude that the 6.13 MeV cascade transition cannot be excluded from the analysis. The ^{16}O structure information from literature [37] do not indi-

[3] In fact, it was claimed [24] that the fit at some beam energies could be improved by including this transition in the analysis.

Table 1
S factor (in keV b) for the γ-ray cascade transitions through the 6.05, 6.13, 6.92, and 7.12 MeV states and the ground state transition. The 6.05 MeV and ground state transition are split in E1 and E2 contributions (see text). Note only the results for the fits including a 6.13 MeV amplitude are listed here. The quoted uncertainties include statistical errors and uncertainties arising from the fit. The energy is defined as in [20], i.e. effective energy in the center of the gas target, with an uncertainty of less than 2 keV [36]. The effect of the energy uncertainty on the S factor is negligible. Systematic uncertainties, e.g. from simulation and total cross section measurement [20], are not included.

E (MeV)	$S^{E2}_{6.05}(E)$	$S^{E1}_{6.05}(E)$	$S_{6.13}(E)$	$S_{6.92}(E)$	$S_{7.12}(E)$	$S^{E2}_{gs}(E)$	$S^{E1}_{gs}(E)$	χ^2_{red}
3.30	2.7 ± 0.4	< 0.7	1.2 ± 0.4	20.4 ± 0.7	1.6 ± 1.1	2.1 ± 0.1	< 0.2	1.21
3.50	3.0 ± 0.2	< 0.3	1.2 ± 0.2	2.6 ± 0.3	1.9 ± 0.3	2.2 ± 0.1	$0.1^{+0.2}_{-0.1}$	1.27
3.80	3.3 ± 0.5	< 0.7	1.7 ± 0.3	2.7 ± 0.4	2.4 ± 0.4	4.4 ± 0.2	$0.1^{+0.3}_{-0.1}$	1.28
4.20	7.7 ± 2.3	< 0.3	3.9 ± 0.6	4.8 ± 0.3	4.5 ± 0.3	36.2 ± 0.3	0.8 ± 0.8	1.06
4.30	19.1 ± 1.5	$0.3^{+1.8}_{-0.3}$	9.9 ± 1.5	10.7 ± 1.3	6.1 ± 1.3	193.8 ± 1.0	$0.5^{+0.8}_{-0.5}$	1.37
4.43	1.3 ± 1.3	2.6 ± 1.9	6.8 ± 1.1	2.6 ± 0.8	5.1 ± 0.8	160.0 ± 0.8	< 0.9	1.38
4.50	1.3 ± 1.0	< 0.6	2.7 ± 0.6	1.1 ± 0.6	2.9 ± 0.5	43.3 ± 0.7	1.0 ± 0.4	0.99

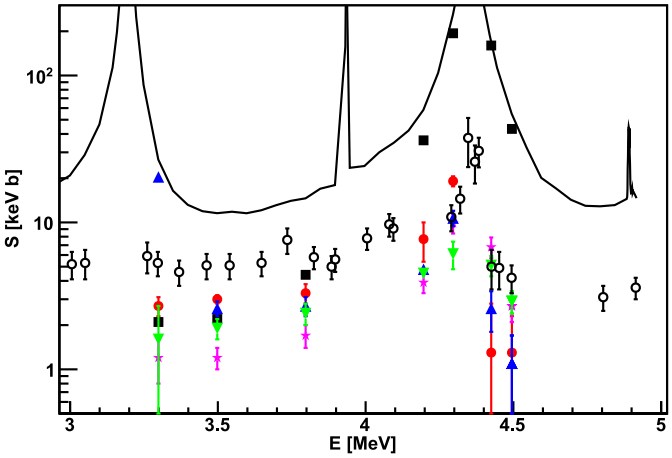

Fig. 3. The astrophysical S factor of the transition in $^{12}C(\alpha,\gamma)^{16}O$ from the present work. Displayed are the transitions to the 6.05 MeV (E2 only, red filled circles), 6.13 MeV (purple stars), 6.92 MeV (blue triangles up), 7.12 MeV (green triangles down) states, and the ground state transition (E2 only, black squares). For comparison the data from [24] are shown (open circles) as well as the total $^{12}C(\alpha,\gamma)^{16}O$ S factor from [20] (black line to guide the eye). (For interpretation of the references to color in this figure legend, the reader is referred to the web version of this Letter.)

cate a strong 6.13 MeV cascade contribution in the energy region studied. However, the available experimental data are rather old and often not published in all experimental details. As a consequence these early experiments might not have the sensitivity to resolve a 6.13 MeV contribution from the other cascade transitions and, therefore, it is not surprising that the literature information is probably incomplete for the present case.

Another important result of the present experiment is that the 6.05 MeV amplitude is almost entirely E2 capture (Table 1) in contrast to the results of the R-matrix calculation from [24] with a dominating E1 contribution over the entire energy region. The published data of [24] reveal no information on the E2/E1 ratio. However, a strong E2 contribution is in agreement with a recent theoretical study of the 6.05 MeV transition [38].

The astrophysical S factor data for all observed transitions are displayed in Fig. 3 and listed in Table 1. In the overlapping energy interval the present 6.05 MeV transition data show a similar energy dependence with respect to the DRAGON data [24], but the absolute scale is about 50% lower. This discrepancy is mainly due to the strength of the 6.13 MeV transition. Indeed, the sum of the 6.05 and 6.13 MeV amplitude results in S factor values very close to the DRAGON data. Moreover, the present 6.13 MeV data exhibit a clear resonance structure around the 2^+ resonance with a smooth energy dependence while the 6.05 MeV transition shows the expected interference structure, e.g. a destructive pattern on the high energy side of this resonance [24] where $S_{6.13}(E) > S_{6.05}(E)$. In particular no larger scattering was observed as one would expect in case the 6.13 MeV amplitude arises from analysis artefacts.

Note that at energies around $E \approx 5$ MeV the primary to the 6.05 MeV state as well as primary and secondary of the 6.13 MeV transition, respectively, have approximately the same γ-ray energy. As a consequence in inverse kinematics experiments the different components cannot be distinguished in the γ-ray spectra due to the large Doppler shift. Therefore, data points here are questionable and this energy region is almost inaccessible for a precise analysis of the cascade transitions.

4. R-matrix analysis of the 6.05 MeV transition

The 6.05 MeV S factor data have been analyzed in the R-matrix formalism. The corresponding R-matrix code was developed specifically for an analysis of the $^{12}C(\alpha,\gamma)^{16}O$ reaction and is based on an alternative parametrization [39] of the original R-matrix theory [40]. The code can use physical resonance parameters [39] and is suited to fit simultaneously the direct γ-ray data, the ^{16}N β-delayed α decay, and the (α,α) elastic scattering, respectively. The details on the code and further results will be published elsewhere [41].

In the analysis the fit was restricted to the present 6.05 MeV direct γ-ray data and the $l=0$ and $l=2$ phase shift data from [16]. The present data predominantly show E2 multipolarity and, therefore, the fit of the γ-ray data was based on $l=2$ capture only. This includes the $J^\pi = 2^+$ subthreshold state, three 2^+ resonances at $E = 2.68$, 4.36 and 5.86 MeV, a background pole, and direct capture. The resonance parameters, i.e. resonance energy, γ and α width, were fit parameters except for the narrow 2.68 MeV resonance where a fixed γ width $\Gamma_{\gamma,6.05}(2.68) = 1.9$ MeV [37] was used. In general, the resonance energies and α widths are basically fixed by the $l=2$ phase shift. The results of the present fit are in good agreement with the values published in [42]. The E2 direct capture contribution is determined by the reduced α width $\gamma_{6.05}$ of the 6.05 MeV subthreshold state. This reduced width is strongly constrained by the $l=0$ elastic scattering phase shift and the R-matrix analysis resulted in a best fit of $\gamma_{6.05} = 0.01^{+0.05}_{-0.01}$ MeV$^{1/2}$ in perfect agreement with a previous analysis [42]. In the simultaneous fit to capture and elastic scattering data the extrapolated astrophysical S factor $S_{6.05}(300)$ spans a large range. Primarily this is caused by the insensitivity of the fit to the interference pattern between DC and subthreshold state. As an example in Fig. 4 two fits with almost identical reduced χ^2 of $\chi^2_{red} \approx 0.7$ but different interference pattern are presented together with the present data. However, tests with all possible interference pattern never resulted in values larger than $S_{6.05}(300) \approx 1$ keV b including all uncertainties from the fit procedure. Therefore, we claim an upper limit of $S_{6.05}(300) < 1$ keV b for this transition. Larger values can only

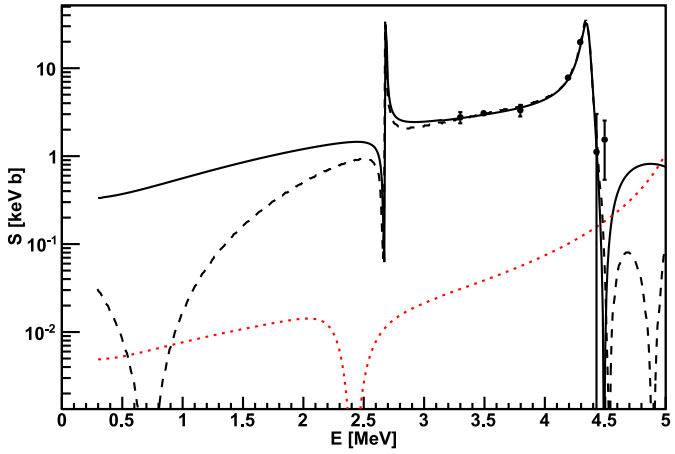

Fig. 4. The R-matrix analysis of the 6.05 MeV transition. The filled circles show the present 6.05 MeV data (E2 only). The black solid and dashed lines represent two best fits with identical χ^2 but different interference pattern. The red dotted line is a R-matrix calculation of the E1 component (see text for details). (For interpretation of the references to color in this figure legend, the reader is referred to the web version of this Letter.)

be retrieved with a significant larger direct capture contribution presently excluded by the elastic scattering data. Note the small E1 contribution in the studied energy region is not in contradiction with E1 contributions from known 6.05 MeV strengths [37] of two 1^- resonances at $E = 5.28$ and 5.93 MeV and their interference with the high energy tail of the $E_x = 7.12$ MeV subthreshold 1^- resonance. Fig. 4 shows the calculation where the interference pattern were chosen to maximize $S_{\mathrm{E1},6.05}(300)$. The strong rise of the E1 component towards lower energies reported in [24] cannot be verified in the present study: the E1 contribution to $S_{6.05}(300)$ remains negligible.

5. Summary

In conclusion, the 6.05 MeV cascade transition in $^{12}\mathrm{C}(\alpha,\gamma)^{16}\mathrm{O}$ was studied with the ERNA recoil separator by means of γ-ray-recoil coincidences, delivering background-free γ-ray spectra in the energy region above $E \geqslant 3.3$ MeV. This energy region gives strong constraints on the extrapolation of the astrophysical S factor for this transition and an R-matrix analysis of the present data yielded an upper limit of $S_{6.05}(300) < 1$ keV b. The large $S_{6.05}(300)$ value found previously [24] is excluded by the present data and R-matrix analysis. We conclude from the present work that the 6.05 MeV cascade transition in $^{12}\mathrm{C}(\alpha,\gamma)^{16}\mathrm{O}$ has no astrophysical relevance at stellar helium burning temperatures.

Acknowledgements

The authors thank C. Rolfs and H.-P. Trautvetter for fruitful discussions. This work was supported by DFG (Ro429/35) and INFN.

References

[1] G. Imbriani, M. Limongi, L. Gialanella, F. Terrasi, et al., Astrophys. J. 558 (2001) 903.
[2] T. Rauscher, A. Heger, R.D. Hoffman, S.E. Woosley, Astrophys. J. 576 (2002) 323.
[3] A. Chieffi, M. Limongi, Astrophys. J. 608 (2004) 405.
[4] C. Tür, A. Heger, S.M. Austin, Astrophys. J. 671 (2007) 821.
[5] C. Tür, A. Heger, S.M. Austin, Astrophys. J. 718 (2010) 357.
[6] I. Dominguez, P. Höflich, O. Straniero, Astrophys. J. 557 (2001) 279.
[7] T.S. Metcalfe, M. Salaris, D.E. Winget, Astrophys. J. 573 (2002) 803.
[8] O. Straniero, I. Dommguez, G. Imbriani, L. Piersanti, Astrophys. J. 583 (2003) 878.
[9] P.G. Prada Moroni, O. Straniero, Astron. Astrophys. 466 (2007) 1043.
[10] C. Rolfs, W. Rodney, Cauldrons in the Cosmos, University of Chicago Press, 1988.
[11] J.M.L. Quellet, M.N. Butler, H.C. Evans, H.W. Lee, et al., Phys. Rev. C 54 (1996) 1982.
[12] R. Kunz, M. Jaeger, A. Mayer, J.W. Hammer, et al., Phys. Rev. Lett. 86 (2001) 3244.
[13] L. Gialanella, D. Rogalla, F. Strieder, S. Theis, et al., Eur. Phys. J. A 11 (2001) 357.
[14] M. Assuncäo, M. Fey, A. Lefebvre-Schuhl, J. Kiener, et al., Phys. Rev. C 73 (2006) 055801.
[15] M. Fey, Ph.D. thesis, Universität Stuttgart, Germany, 2004.
[16] P. Tischhauser, A. Couture, R. Detwiler, J. Görres, et al., Phys. Rev. C 79 (2009) 055803.
[17] R.E. Azuma, L. Buchmann, F.C. Barker, C.A. Barnes, et al., Phys. Rev. C 50 (1994) 1194.
[18] R.H. France III, E.L. Wilds, J.E. McDonald, M. Gai, Phys. Rev. C 75 (2007) 065802.
[19] X.D. Tang, K.E. Rehm, I. Ahmad, C.R. Brune, et al., Phys. Rev. Lett. 99 (2007) 052502.
[20] D. Schürmann, A. Di Leva, L. Gialanella, D. Rogalla, et al., Eur. Phys. J. A 26 (2005) 301.
[21] K.U. Kettner, H.W. Becker, L. Buchmann, J. Görres, et al., Z. Phys. A 308 (1982) 73.
[22] A. Redder, H.W. Becker, C. Rolfs, H.P. Trautvetter, et al., Nucl. Phys. A 462 (1987) 385.
[23] L.R. Buchmann, C.A. Barnes, Nucl. Phys. A 777 (2006) 254.
[24] C. Matei, L. Buchmann, W.R. Hannes, D.A. Hutcheon, et al., Phys. Rev. Lett. 97 (2006) 242503.
[25] J.D. Larson, R.H. Spears, Nucl. Phys. A 56 (1964) 497.
[26] D. Rogalla, D. Schürmann, F. Strieder, M. Aliotta, et al., Nucl. Instr. Meth. A 513 (2003) 573.
[27] L. Gialanella, D. Schürmann, F. Strieder, A. Di Leva, et al., Nucl. Instr. Meth. A 522 (2004) 432.
[28] D. Schürmann, F. Strieder, A. Di Leva, L. Gialanella, et al., Nucl. Instr. Meth. A 531 (2004) 428.
[29] D. Rogalla, M. Aliotta, C.A. Barnes, L. Campajola, et al., Eur. Phys. J. A 6 (1999) 471.
[30] A. Di Leva, L. Gialanella, R. Kunz, D. Rogalla, et al., Phys. Rev. Lett. 102 (2009) 232502.
[31] A. Di Leva, M. de Cesare, D. Schürmann, N. de Cesare, et al., Nucl. Instr. Meth. A 595 (2008) 381.
[32] A. Ordine, A. Boiano, E. Vardaci, A. Zaghi, A. Brondi, IEEE Trans. Nuclear Sci. 45 (1998) 873.
[33] Geant4 Collaboration, S. Agostinelli, et al., Nucl. Instr. Meth. A 506 (2003) 250.
[34] D. Schürmann, Ph.D. thesis, Ruhr-Universität Bochum, Germany, 2007.
[35] F.C. Barker, T. Kajino, Aust. J. Phys. 44 (1991) 369.
[36] H.W. Becker, M. Bahr, M. Berheide, et al., Z. Phys. A 351 (1995) 453.
[37] D.R. Tilley, H.R. Weller, C.M. Cheves, Nucl. Phys. A 564 (1993) 1.
[38] M. Dufour, P. Descouvemont, Phys. Rev. C 78 (2008) 015808.
[39] C.R. Brune, Phys. Rev. C 66 (2002) 044611.
[40] A.M. Lane, R.G. Thomas, Rev. Mod. Phys. 30 (1958) 257.
[41] R. Kunz, D. Schürmann, et al., 2011, in preparation.
[42] P. Tischhauser, R.E. Azuma, L. Buchmann, R. Detwiler, et al., Phys. Rev. Lett. 88 (2002) 072501.